Individual variability in behavior and functional networks predicts vulnerability using a predator scent model of PTSD

Pablo D. Perez[#1], David Dopfel[#1], Hector Bravo-Rivera [2], Gregory J. Quirk[2], Nanyin Zhang*[1]

[1]Department of Biomedical Engineering, Pennsylvania State University, University Park, PA, USA
[2]Departments of Psychiatry and Anatomy & Neurobiology, University of Puerto Rico School of Medicine, San Juan, Puerto Rico

#: These authors contributed equally to this work.

***Address for correspondence:**

Nanyin Zhang, Ph.D

Professor of Biomedical Engineering and Electrical Engineering

The Huck Institutes of Life Sciences

The Pennsylvania State University

W-341 Millennium Science Complex, University Park, PA 16802, USA

Email: nuz2@psu.edu

Key words: Post-traumatic Stress Disorder; Vulnerability; Resilience; Rat; Resting-state fMRI

Abstract:

Only a minority of individuals who experience traumatic event(s) subsequently develop post-traumatic stress disorder (PTSD). However, whether differences in vulnerability to PTSD result from predisposition or a consequence of trauma exposure remains unclear. A major challenge in differentiating these possibilities is that clinical studies focus on individuals already exposed to traumatic experiences, and do not take into account pre-trauma conditions. Here using the predator scent model of PTSD in rats and a longitudinal design, we measured pre-trauma brain-wide neural circuit functional connectivity (FC), behavioral and corticosterone responses to trauma exposure, and post-trauma anxiety. Individual differences in freezing responses to predator scent exposure correlated with differences in pre-trauma FC in a set of neural circuits, especially in olfactory and stress-related systems, indicating that pre-existing function in these circuits could predispose animals to differential fearful responses to threats. Counterintuitively, rats with the lowest freezing showed more avoidance of the predator scent, a blunted corticosterone response, and higher anxiety long after exposure. This study provides a comprehensive framework of pre-existing circuit function that determines threat response strategy, which might be directly related to the development of PTSD-like behaviors.

Introduction

Maladaptive response to trauma may lead to chronic stress disorders like posttraumatic stress disorder (PTSD). While trauma exposure is a feature of PTSD, it is not an unequivocal predictor of the disorder. In fact, only a minority of individuals who experience traumatic event(s) subsequently develop PTSD. However, mechanisms underlying this individual difference in vulnerability remain unclear.

It has been suggested that vulnerability to PTSD may result from individual differences in early life events, preexisting conditions, or responses to trauma exposure [1-3]. However, mixed results have been reported. For instance, reduced hippocampal volume has long been considered a marker of PTSD. Nevertheless, some studies suggest that PTSD-related decreases in hippocampal volume might be a consequence of traumatic events and PTSD development, whereas other studies showed that PTSD patients' twins who did not have a trauma experience also had smaller hippocampal volumes, suggesting that reduced hippocampal volume may pre-dispose individuals to developing PTSD [4-7]. These conflicting results are also reported in studies of cortisol levels and brain activity in relation to PTSD [8-10], which together contribute to our elusive understanding of individual vulnerability to PTSD.

A major obstacle of investigating risk factors of PTSD is rooted in the difficulty of longitudinally monitoring of PTSD development pre- through post-trauma in humans with well-controlled traumatic events. Studies in humans focus on populations already exposed to a variety of uncontrolled traumatic events [11]. Such barriers can be overcome in experimental animals, for which a longitudinal design with controlled traumatic stressors can be conveniently applied. Among many stress paradigms that have been

used to produce rat models of PTSD, predator scent exposure in an inescapable environment is a commonly used psychological stressor [12]. This method mimics a life-threatening situation that is ecologically relevant and physically innocuous, preventing confounding effects of inflammation or pain due to injury. Recent work with this model has found that PTSD-like behaviors are exhibited following exposure to predator scent [13]. Importantly, Cohen et al. distinguished the responses of mal- vs. well-adapted rats, showing a 25-30% prevalence of PTSD-like behavior in rats exposed to trauma [14]. This work highlights the potential for this animal model to investigate relevant individual variability in PTSD-like responses to trauma. Missing from previous studies, however, is information about preexisting conditions of animals that might predict their immediate and long-term responses to trauma.

Additionally, little is known about whether and how specific defense responses to a threat correlate with susceptibility to maladaptation. Exposure to a stressor elicits different fear responses depending on the perceived proximity and intensity of the threat. Moderate stressors produce passive freezing, while imminent predation threats elicit a fight or flight response [15,16]. However, whether behavioral responses to predator odor is a useful indicator of subsequent development of PTSD is unknown.

Here we employed a longitudinal approach to studying individual variability of behavioral and functional outcomes of the predator scent animal model of PTSD. Resting-state functional magnetic resonance imaging (rsfMRI) data were collected from awake rodents before trauma exposure to record pre-existing neural circuit function using the awake rat rsfMRI approach established in our lab [17-20]. Awake rat rsfMRI avoids confounding factors from anesthetics and permits correlation with behavior [21-23].

We found that individual differences in behavior and neural circuit function prior to trauma exposure predicted animals' susceptibility to developing PTSD-like behaviors. This suggests that pre-existing traits such as anterior olfactory nucleus (AON)-amygdala connectivity may be critical for determining individual resilience/susceptibility to developing PTSD.

Results

The experimental schedule was summarized in Fig 1a. Rats were first scanned using rsfMRI, then exposed to fox urine, and then given an anxiety test approximately one week after exposure.

Freezing responses to fox urine were highly variable across animals

A total of 87 Long-Evans (LE) rats were exposed to a predator scent stressor in the form of a compressed cotton pad sprayed with fox urine in an inescapable cage for 10 min. Freezing and location within the cage were quantified with behavioral tracking software (ANY-maze, Stoelting Co., Reston, VA). Compared to control animals that were exposed to a clean cotton pad, the group exposed to predator scent showed increased freezing (t-test, $t_{87} = 3.660$, $p = 0.00044$, Fig. 1b, left), and maintained a significantly greater distance from the cotton pad (t-test, $t_{87} = 3.568$, $p = 0.00060$, Fig. 1b, right). These data confirm that predator scent exposed animals displayed a significantly greater stress response compared to controls.

Closer examination of animals' freezing time revealed distinct frequency distributions between groups. Fig. 1c shows the histograms of freezing time in both

groups. Control animals exhibited a unimodal distribution of freezing, whereas predator scent exposed animals displayed large inter-subject variability with a bimodal distribution (Fig. 1c, right panel) fitted with a mixed Gaussian distribution (bimodal Gaussian function provided the best fit relative to uni-modal and tri-modal Gaussian functions, model fit quality (the model with the lowest AIC is the best model to fit the data): Δ_1(AIC) = 11, Δ_2(AIC) = 0, Δ_3(AIC) = 6; Akaike weight for each model: w_1 = 0.0039, w_2 = 0.947, w_3 = 0.0488). To further investigate this variation in freezing behavior, predator scent exposed animals in the top and bottom tertiles of freezing time were separated into high-freezing and low-freezing subgroups, respectively (n = 21 for each subgroup). Fig. 1d plotted freezing time as a function of exposure time in high-freezing, low-freezing and control groups. Interestingly, it was found that freezing differed between high- and low-freezing animals even during the first minute of predator scent exposure (two sample t-test, $p < 0.009$) and this difference became larger over the time course of the exposure. There was no difference between low-freezing rats and controls. There was also no significant difference in mobility among all three groups, as evidenced by the maximum speed during exposure (one-way ANOVA, $F_{(2, 62)} = 0.86$, $p = 0.43$, Supplement Figure 1).

Low-, but not high-freezing animals were susceptible to developing PTSD-like behaviors

The fact that freezing time was almost identical between low-freezing and control animals might suggest that low-freezing animals had a similar stress response to controls. However, the spatial distribution of time spent in the cage during exposure to predator scent suggested a different interpretation (Fig. 2). Control animals did not show

a side preference with a near normal distribution of the time spent close to the center of the cage (Fig. 2a). In contrast, both high and low freezing animals exhibited a leftward skewed distribution of time spent, farther away from the fox urine. The average distance from the cotton pad was significantly greater in both low- and high-freezing animals compared to controls (One-way ANOVA, $F_{(2, 62)} = 10.97$, $p = 0.000050$ and $p = 0.031$, respectively), indicating avoidance behavior in exposed animals. This difference was also supported by the normalized freezing time at different distances from the cotton pad, as shown in Fig. 2b. Similar to the distribution of the total time spent in the cage, control animals did not seem to have any preference for the side of the cage in which they froze, whereas both high- and low-freezing animals tended to freeze farther away from the fox urine sample. Relative to high-freezing animals, low-freezing animals showed even more leftward bias as reflected by significantly less freezing time in the zone 24 cm away from the pad (repeated measures ANOVA, $F_{Group \times Zone}(22, 682) = 3.00$, $p = 0.0000059$; tukey-cramer post-hoc test, low- vs high-freezing at 24 cm: $p = 0.04$), indicating that low-freezing animals were somewhat more avoidant than high-freezing animals. This can also be seen in the heat plots of Fig. 2a. Prior to predator scent exposure during the acclimation period, the three groups showed no significant differences in freezing time (One-way ANOVA, $F_{Group \times Zone}$ $(2, 62) = 0.24$, $p = 0.78$, Supplement Figure 2) or location distribution (the cage was divided into three even-size zones, Two-way ANOVA, $F_{Group \times Zone}(4, 186) = 1.28$, $p = 0.28$).

To assess the long-lasting PTSD-like behaviors in exposed animals, we measured anxiety level using elevated-plus maze (EPM) 6 days after predator scent exposure. Resembling the observation of increased avoidance, low-freezing animals

also exhibited heightened long-lasting anxiety compared to both control (t-test, $t = 2.24$, $p = 0.030$) and high-freezing animals (t-test, $t = 3.37$, $p = 0.0017$), as indicated by the ratio of open/open+close arm time in EPM tests (Fig. 2c). There was no statistical difference between high-freezing and control animals, indicating that low-, but not high-freezing animals were susceptible to developing PTSD-like behaviors following exposure to predator scent. In addition, freezing was positively correlated with the EPM score in exposed animals ($R^2 = 0.21$, $p = 0.0002$), but not controls ($R^2 = 0.01$, $p = 0.62$, Fig. 2d). These results demonstrate that behavioral responses during trauma exposure can predict long-term maladaptation.

Low-freezing animals showed blunted corticosterone response to predator scent

In a subset of the animals (n=12), corticosterone (CORT) level was measured immediately before predator scent exposure as well as 30 min, 60 min and 120 min after exposure (Fig. 3). Again, we segregated rats according to their freezing time during predator scent exposure using the same cutoff values from the main cohort of animals described above and found similarly distributed populations of high- (n = 3) and low- (n = 4) freezing subgroups. The low-freezing animals exhibited a blunted CORT response compared to the high-freezing and control animals. Specifically, we quantified the CORT responsiveness by taking into account both the rise and fall around the peak hormonal response (30 min) (i.e. absolute CORT change from 0 to 30 min + absolute CORT change from 30 to 60 min). High- and low-freezing animals showed a significant difference in the CORT responsiveness (Fig. 3c, t-test, $t = 2.73$, $p = 0.043$). In addition, the CORT response to exposure was linked to long-lasting anxiety level, as evidenced

by a significant correlation with the EPM score measured 6 days after exposure (R^2 = 0.56, p = 0.05, Fig. 3b).

Pre-trauma neural circuit functional connectivity predicted fear responses.

In addition to behavioral tests, rsfMRI was performed before trauma exposure to measure preexisting resting-state functional connectivity (RSFC) in neural circuits across the whole brain. Echoing our behavioral data showing difference in freezing during the very beginning of predator scent exposure, RSFC of multiple widespread neural circuits significantly differed between high- and low-freezing animals (false discovery rate (FDR) = 0.01, Supplement Figure 3A). These regions/circuits have been implicated in stress responses, processing of emotionally valent stimuli, olfactory function and freezing behavior.

To identify the specific neural circuits correlated with the freezing phenotype, we conducted a data-driven correlational analysis for all neural connections (67 regions covering the whole brain, 2211 connections in total) between their RSFC and the cumulative freezing time across all exposed animals. 15 neural circuits exhibited a significant correlation between pre-exposure RSFC and freezing time ($p < 0.05$, FDR corrected, Fig. 4). Relative to high-freezing animals, six of these connections showed stronger connectivity, whereas 9 showed lower connectivity in low-freezing animals, suggesting that the pre-trauma activity within these circuits might have predictive value for the freezing behavior during exposure. The diagram of this freezing-associated network was summarized in Fig. 5.

A closer examination of these 15 circuits revealed a comprehensive network particularly involving the olfactory and stress-related brain areas. Specifically, low-freezing animals showed stronger pre-trauma connectivity in two olfactory circuits (i.e. AON-amygdala, and olfactory bulb-auditory cortex), two septal circuits (i.e. lateral septum (LS)-bed nucleus of the stria terminalis (BNST), medial septum (MS)-prelimbic cortex (PL)), and two circuits within the stress system (lateral hypothalamus-cortical amygdala and lateral hypothalamus-amygdala). Stronger connectivity in the two olfactory circuits suggest that odor may exert more influence on the amygdala and cortex in low-freezing animals. Additionally, the LS-BNST projection might underlie stronger predator scent-induced stress response in low-freezing animals. In support of this, both the LS and BNST are activated by predator odor [24,25], and the BNST is actively involved in sustained fear response to diffuse threat [26]. Stronger functional connectivity within the stress system can also contribute to higher stress response and anxiety in low freezing animals.

Conversely, nine neural circuits showed weaker pre-trauma functional connectivity in low-freezing animals, including two parabrachial nucleus (PBn) circuits (PBn-BNST and PBn-hypothalamus), two nucleus accumbens (NAc) circuits (NAc-amygdala and NAc-visual cortex), two zona inserta (ZI) circuits (ZI-pituitary gland and ZI-visceral cortex), as well as the circuits of lateral olfactory tract nucleus (nLOT)-anterior cingulate cortex (ACC), postsubiculum-agranular insula (AI), and globus pallidus (GP)-paraventricular (PVN) hypothalamus. PBn is tightly related to olfactory function and electrophysiological data show that calcitonin gene–related peptide (CGRP) in PBn has inhibitory effects in the BNST [27]. Therefore, weaker connectivity in

the PBn-BNST circuit suggests less inhibition in BNST and could contribute to heightened anxiety in low freezing animals. Weaker RSFC between the nLOT and ACC can reduce ACC's control over predator scent-triggered defense reaction in low-freezing animals. In addition, decreased NAc connectivity was consistent with report of the inverse association between NAc activity and the intensity of emotional stress response [24], which might also be related to goal-directed motor behavior [28]. Furthermore, lower connectivity in ZI circuits (i.e. ZI-pituitary gland and ZI-visceral cortex) may be involved in control of sympathetic visceral reactions and the hypothalamus–pituitary–adrenal (HPA) axis activity [29], consistent with blunted CORT response in low-freezing animals. Lastly, the GP-PVN hypothalamus projection, known to involve corticotropin-releasing factor (CRF) neurons, were reported to link stress response to motor output [30].

Taken together, these data indicate that differences in functional connectivity in neural circuits particularly involving the olfactory and stress-related systems might predispose animals to differential stress responses during predator scent exposure, which can be linked to individual difference in subsequent development of PTSD-like behaviors long after trauma exposure.

Differential fear behavior during exposure and long-term anxiety between low- and high-freezing animals were not induced by pre-exposure imaging itself.

To rule out the possibility that differential fear response during predator scent exposure and long-term anxiety between low- versus high-freezing animals indeed resulted from predator scent exposure as oppose to other factors such like the imaging

procedure, we also divided control animals into tertiles based on their cumulative freezing time. No differences in avoidance behaviors including distance to the cotton pad (two-sample t-test, $t = 1.22$, $p = 0.25$), the distribution of time spent in the cage (two-way ANOVA, $F_{2,28} = 2.20$, $p = 0.13$, also see Supplement Figure 4), the distribution of freezing time in the cage (repeated measures ANOVA, $F_{2,154} = 0.34$, $p = 0.98$), or long-term anxiety level (EPM score, two-sample t-test, $t = 0.37$, $p = 0.72$) were observed between low- and high-freezing control animals. In addition, unlike predator scent-exposed animals, no neural connections exhibited correlation between pre-exposure RSFC and freezing time, and no connection displayed significant RSFC difference between low- and high-freezing control animals (Supplement Figure 3B), indicating that these animals had virtually no difference in neural circuit function. These results collectively confirmed that differential fear behavior and long-term aftereffect between low- and high-freezing animals were not driven by the imaging procedure or any other factors because all control animals underwent the identical procedures including imaging, except for being exposed to predator scent.

Discussion

Employing a longitudinal design, we investigated animals' individual variability in stress response and subsequent development of PTSD-like behaviors following predator scent exposure. We found that animals exhibited large differences in freezing behavior during fox urine exposure. Animals expressing less freezing exhibited increased avoidance and tended to develop long-lasting heightened anxiety. Importantly,

this difference in behavioral responses was apparent at the beginning of predator scent exposure, suggesting pre-existing vulnerability. This notion was supported by the rsfMRI data showing significant pre-trauma difference in neural circuit connectivity between high- and low-freezing animals. In addition, low-freezing animals showed blunted CORT response to predator scent, which was correlated with EPM anxiety measurement. Taken together, this study provides important evidence supporting the hypothesis that preexisting circuit function determines the defense response strategy during threat and that this behavioral response might be directly related to the development of PTSD. It also highlights the importance of studies that analyze factors both before and after trauma for the study of PTSD.

Freezing time alone might not be a reliable measure of response to threat.

Behavioral response to stress is commonly categorized into fight, flight or freezing. In rodent behavior testing, freezing time is often used as the dominant measure of threat reaction. Although freezing is a universal fear response, it manifests at intermediate levels of predator threat [16]. Meanwhile, other types of threat-induced responses including fight-or-flight, which is elicited during imminent threat [15], and avoidance can counteract the measure of freezing. For this reason, utilizing freezing time as the only measure for stress response of an individual animal can be problematic if alternative coping strategies are not considered [31]. Indeed, there is growing evidence suggesting the ambiguity of freezing time as it relates to stress [15,32].

In line with this concept, our data show that animals with the lowest freezing time are in fact the most stressed subgroup. Their highly biased distribution in the total time and freezing time at different distance to the cotton pad indicate that low-freezing animals might have perceived a higher threat level and used strategies other than freezing (e.g. avoidance), particularly at closer proximity to the pad. This higher perceived threat level is likely a crucial factor in maladaptation to stress response (e.g. higher long-lasting anxiety level), which is in line with the literature investigating the role of threat perception in human PTSD diagnoses [33]. In addition, in low-freezing animals, the CORT response was blunted and had a delayed recovery back to baseline after stress, and this pattern of CORT response has also been suggested as a marker of maladaptation to stress in PTSD [34,35]. Our CORT data is also consistent with the theory that stress hormone production is an important and protective part of an acute stress response triggering negative feedback on CORT production [36,37]. Taken together, these results demonstrate that freezing time alone might not be a reliable measure of reaction to threat. These data also highlight the importance of separating subpopulations, in particular in stress studies, as information can be lost through the averaging of subpopulations that display bidirectional responses.

Behavioral and neuroendocrine reactions to a threat predict susceptibility to long-term maladaptation

Whether defensive reactions predict long-term emotion regulation and symptom development has been an unresolved issue, largely due to lack of longitudinal studies that follow up the relationship between behavioral reactions during trauma exposure

and the development of psychopathology [15]. Our longitudinal study demonstrates that freezing during trauma exposure predicts long-term maladaptation in animals, supporting that specific behavioral responses to a threat might predict susceptibility to long-term PTSD-like behaviors.

The relationship between the behavioral reaction during stress and vulnerability to stress maladaptation is corroborated by neuroendocrine measure during and following predator scent stress. We observed that low-freezing (i.e. vulnerable) animals had blunted CORT response relative to high-freezing (resilient) animals, and this CORT response was also correlated to the EPM measure 6 days later. These data are consistent with the literature reporting that blunted CORT response to predator scent predicts avoidance in rats [38]. This linkage between lower levels of HPA axis activity immediately after stress and vulnerability to subsequently develop PTSD has also been repeatedly reported in humans [39,40], suggesting that this relationship might represent a general phenomenon mammals. Conversely, higher glucocorticoid receptor expression was associated with resilience to stress [41]. Taken together, our data indicate that individual variation in behavioral and hormonal responses to stress can be key predictors of the development of emotion regulation and chronic pathological states.

Pre-trauma neural circuit function predisposes animals to differential stress response.

i) Connections between the olfactory and stress systems

Our rsfMRI data suggest that sensory inputs play an important role in the stress response and subsequent development of PTSD-like behaviors. AON has been shown

to be activated by variable stressors [42] including predator scent [43]. The mitral/tufted (MT) cells in the olfactory bulb send their processes to AON [44], which projects to amygdala [45]. This connectivity suggests that the flow of olfactory information through the AON to the amygdala could drive the stress response to predator scent. Stronger AON-amygdala connectivity in low-freezing animals suggest that the olfactory cue could have a stronger impact on amygdala activity, which would lead to stronger stress response. Conversely, weaker nLOT-ACC connectivity in low-freezing animals indicates less ACC control during predator scent exposure, which can affect the switching between freezing and active defense modes [46]. These data also agree with the report that the olfactory cortex and its connections with the stress system are tightly linked to stress hormone responses to predator scent in rodents [47]. Taken together, these results highlight the importance of sensory input in the stress response during predator scent exposure.

In addition to stronger sensory-stress connectivity, stronger functional connectivity within the stress system was observed in low-freezing animals, consistent with their higher stress response and anxiety. In particular, it is known that threat-induced autonomic sympathetic responses are mediated by amygdala projections to the lateral hypothalamus [15]. Stronger connectivity in this circuit suggests that low-freezing animals might have higher arousal, higher cardiovascular activity and increased muscle tone during predator odor exposure [48].

ii) BNST circuits

Our data also demonstrated that BNST is involved in the neural network associated with differential stress responses during predator scent exposure. BNST, as a part of extended amygdala, is well known to be involved in sustained anxiety when a

threat is diffuse and/or uncertain [26,49] such as predator odor [25]. As a result, this region is particularly associated with anxiety [50-52]. The anatomical connection in BNST-LS and BNST-PBn have been well documented [27,53,54], but the specific function of these projections is less well studied. It has been shown that CGRP in the PBn inhibits neurons of the BNST [27], and BNST projections to the PBn dampen anxiety response [55]. These data support the idea that weaker PBn-BNST connectivity in low-freezing (i.e. vulnerable) animals caused disinhibition of BNST activity, which led to stronger stress response and heightened long-lasting anxiety. Conversely, LS mediated activity, possibly again driven by olfactory inputs [24], can potentiate BNST activity in these animals, also generating stronger stress response and higher anxiety.

iii) The hypothalamus-GP circuit

Another interesting circuit that is coupled to freezing behavior is the PVN-GP connection. CRF neurons in the PVN hypothalamus, amygdala and BNST send synapses to the external GP [30], which expresses high levels of the primary CRF receptor (i.e. CRFR1). These connections makes GP an entry point connecting the stress system with the basal ganglia, which links the stress-relevant information to the directed movement [30]. Consistent with this notion, our data suggest that the pre-trauma connectivity in this circuit is directly associated with stress-related freezing behavior in animals.

iv) Possible contributions of other neural circuits to variable freezing behavior

Stronger connectivity between the MS and PL can be linked to stronger fear in low-freezing animals, given that PL promotes fear expression [56]. Also considering septal

neurons are known to mediate the generation of theta oscillations [57,58], the MS-PL connection may contribute to fear-associated theta rhythm in prefronto-amygdalo-hippocampal pathways [59]. In addition, the postsubiculum-insula circuit connectivity could be responsible for differential spatial movement in separate subgroups of animals.

Lastly, a number of additional connections showed significant difference in pre-trauma RSFC between low-freezing and high-freezing animals, even though their RSFC was not correlated with freezing time. For example, lower RSFC between CA3 and reticular nucleus (RT) was observed in low-freezing rats. RT is the hub connecting hippocampus with PFC. Reduced connectivity in vulnerable rats might be due to less contribution of hippocampus to PFC control processes [60]. Another possibility is the increased connectivity between CA1 and anterior cingulate area (ACA), which suggests that hippocampus may be driving fear or avoidance via projections to ACA by reporting that the context is unsafe. Although premature, these results suggest that preexisting neural circuit difference in vulnerable animals might compose of a sophisticated network, and PTSD should be viewed as a network phenomenon.

Relevance to human PTSD

Our neural circuitry and neuroendocrine findings in animals echo PTSD research in humans. Altered sensory function has also been reported in PTSD patients [61]. In addition, a significant number of brain regions identified here (e.g. BNST) are tightly related to anxiety disorders in humans [62], although the present study goes beyond static neuroanatomy of individual brain regions and focuses on pre-existing neural circuit

function. Furthermore, human data also suggest that blunted CORT response is a predictor of vulnerability to subsequent development of PTSD [39,40], while adequate and timed CORT rise protects against PTSD [63,64]. Taken together, these results provide compelling evidence demonstrating the relevance of the present study to human PTSD.

In summary, our data demonstrate that differences in neural circuit function present before trauma exposure may predispose animals to specific stress responses and long-term PTSD-like behaviors. Future studies that focus on the causal relationship between the baseline neural circuit function and behavioral responses during trauma exposure and long-term outcome in PTSD-like behaviors will be important in further understanding the specific relationship between these neural circuits and pathological susceptibility and development of PTSD. For instance, it will be of particular interest to test whether optogenetic manipulation of specific pathways based on the rsfMRI data during trauma exposure can alter stress response and development of long-term PTSD-like behaviors in animals.

Methods

Adult male LE rats (250-350g) were obtained from Charles River Laboratories (Raleigh, North Carolina site). Rats were housed in pairs in Plexiglas cages with controlled ambient temperature (22-24 °C) on a 12/12 hour day-dark schedule. Food and water were provided ad libitum. A total of 87 rats were used in the present study, in which 23 rats were controls and 64 rats were exposed to predator scent using a single-episode predator scent exposure in an inescapable environment paradigm. Two rats

were removed from the exposed group before analysis due to health concerns. All rats were used for behavior tests and rsfMRI experiments. All animal procedures were reviewed and approved by the Institutional Animal Care and Use Committee (IACUC) of the Pennsylvania State University. The experimental procedure was summarized in Fig. 1a.

Single-episode predator scent exposure

Rats were exposed to a single episode of predator scent stress in an inescapable environment for 10 min. The day prior to exposure, each rat was assigned to its own exposure cage (i.e. a Plexiglas cage with no bedding) and habituated to the cage environment for 30 min. The cage was left soiled after habituation. On the exposure day, the rat was placed in its corresponding cage for a total of 12 min. After 2 min of adaptation, a cotton pad sprayed with red fox urine was placed at the right end of the cage for another 10 mins (Red fox urine, Wild Life Research Center). The pad was put on a wire mesh inside the cage, right below the lid and out of reach of the rat. The control animal was exposed to the same cotton pad without fox urine. During exposure, the rat was recorded by a video camera. Following predator scent exposure, the rat was returned to his home cage and left undisturbed for 6 days.

Elevated plus maze (EPM)

The EPM test was performed to measure the anxiety level 6 days after trauma exposure. The maze consisted of four perpendicular arms forming a cross and elevated 50 cm from the floor. Two arms were closed, opposed to each other and enclosed by 40-cm high walls. The remaining two arms, also opposed to each other, were

completely open. A camera was placed directly above the maze to record the rat movement.

To perform the test, the rat was initially placed in the center of the maze facing one open arm and allowed to freely explore the maze for 5 min. The times spent in the open and closed arms were determined. The ratio of time in open arms versus that in both open and closed arms [i.e. open/(open+closed)] was calculated to provide a measure of anxiety level. A lower score of this ratio indicates a higher level of anxiety. The maze was cleaned with a 70% alcohol solution in water between tests.

CORT Measurement

A subset of rats (n = 12) had blood samples collected to quantify the hormonal response to stress. Corticosterone (CORT) level was measured immediately before predator scent exposure and 30 min, 60 min, and 120 min after exposure to measure the dynamic response to predator scent stress exposure. Initial blood samples were collected through tail nick, with subsequent time point samples collected by disturbing the tail scab. Samples were collected using heparin coated microtubes with capillary tube inserts (RAM Scientific Safe-T-Fill, Nashville, TN, USA). Samples were centrifuged to obtain plasma and stored at -20 ºC. The plasma CORT level was then quantified using CORT enzyme-linked immunosorbent assay (ELISA) kit (Enzo life sciences Inc. Ann Arbor, MI. Cat ADI-901-097) according to the manufacturer's manual. For simple utilization of the repeated measures, CORT response was quantified by the sum of the absolute change around the peak hormonal response time of 30 min. This measurement is sensitive to the rise and fall of CORT response to stress and therefore representative of the responsiveness of the hormonal system.

Acclimation and rsfMRI data acquisition

All rats were scanned before the trauma-exposure experiment. Before imaging, animals were acclimated to a 'mock' imaging environment for 7 days. This acclimation protocol was employed to diminish the stress and motion of the subject during scans [65]. The rat was first briefly anesthetized with 2-4% isoflurane in oxygen. The head was restrained with a bite bar, nose bar and side pads that restricted the head motion. A pair of shoulder bars and a body tube maintained the body in place without impeding ventilation. Animals were allowed to regain consciousness after being set up in the restrainer, typically in 10 mins. The rat was then placed in a dark ventilated box and the sound of different MRI sequences was played, presenting an environment mimicking MRI scanning. All rats were given 7 daily acclimation sessions with a gradually increasing acclimation period (15, 30, 45, 60, 60, 60 and 60 min from day 1 to day 7). A similar approach has also been applied in several other groups [66-68].

At least 2 days after acclimation, MRI scans were performed in a 7-Tesla scanner interfaced with the Bruker console system (Bruker, Germany). The rat was first briefly anesthetized with 2-4% isoflurane in oxygen and set up in the same restrainer with a built-in birdcage 1H radiofrequency volume coil. Anesthesia was then discontinued, and the rat was allowed to regain consciousness and placed into the MRI magnet bore. rsfMRI data were obtained using single shot gradient-echo echo-planar imaging sequence with the parameters of repetition time (TR) = 1 sec, echo time (TE) = 13.8 ms, 64 × 64 matrix size, 20 slices with 1 mm thickness, field of view (FOV) = 32 × 32 mm^2, in-plane resolution = 500 × 500 μm^2. Each rat was scanned for 2400 EPI volumes per scan session. Anatomical images were also acquired using a fast spin-

echo sequence with the parameters of TR = 1500 ms; TE = 8 ms; matrix size = 256 × 256; FOV = 3.2 × 3.2 cm^2; slice number = 20; slice thickness = 1 mm; RARE factor = 8.

rsfMRI data processing

rsfMRI images were preprocessed by performing alignment using Medical Image Visualization and Analysis (MIVA, http://ccni.wpi.edu/), motion correction using SPM 12 (http://www.fil.ion.ucl.ac.uk/spm/), spatial smoothing (Gaussian kernel: FWHM = 0.75 mm) and temporal smoothing (band-pass filter, cutoff frequencies: 0.01-0.1Hz), and regression of motion parameters and signals from the white matter and ventricles as described in past studies [20,22,23,69]. Before performing these steps, EPI volumes with relative framewise displacement (FD) > 0.2 mm and their immediate temporal neighbors were first removed [70]. In addition, the first 10 volumes of each rsfMRI run were also removed to ensure the magnetization was at steady state.

Functional connectivity analysis was conducted using region-of-interest (ROI) based correlational analysis. This method evaluated the RSFC by quantifying the Pearson correlation coefficient of regionally averaged spontaneous BOLD signals between different brain regions. A linear mixed effect model was used to determine the overall effect on RSFC of each group of rats, while removing any random effect from different batches of animals.

Acknowledgments

The present study was partially supported by National Institute of Neurological Disorders and Stroke Grant R01NS085200 (PI: Nanyin Zhang, PhD) and National

Institute of Mental Health Grant R01MH098003 and RF1MH114224 (PI: Nanyin Zhang, PhD).

Conflict of interest: none.

References:

1 Charney, D. S. Psychobiological mechanisms of resilience and vulnerability: implications for successful adaptation to extreme stress. *Am J Psychiatry* **161**, 195-216, doi:10.1176/appi.ajp.161.2.195 (2004).

2 Yehuda, R. & LeDoux, J. Response variation following trauma: a translational neuroscience approach to understanding PTSD. *Neuron* **56**, 19-32, doi:10.1016/j.neuron.2007.09.006 (2007).

3 Feder, A., Nestler, E. J. & Charney, D. S. Psychobiology and molecular genetics of resilience. *Nat Rev Neurosci* **10**, 446-457, doi:10.1038/nrn2649 (2009).

4 Gilbertson, M. W. *et al.* Smaller hippocampal volume predicts pathologic vulnerability to psychological trauma. *Nat Neurosci* **5**, 1242-1247, doi:10.1038/nn958 (2002).

5 Bonne, O. *et al.* Longitudinal MRI study of hippocampal volume in trauma survivors with PTSD. *Am J Psychiatry* **158**, 1248-1251, doi:10.1176/appi.ajp.158.8.1248 (2001).

6 McEwen, B. S., Nasca, C. & Gray, J. D. Stress Effects on Neuronal Structure: Hippocampus, Amygdala, and Prefrontal Cortex. *Neuropsychopharmacology* **41**, 3-23, doi:10.1038/npp.2015.171 (2016).

7 Logue, M. W. *et al.* Smaller Hippocampal Volume in Posttraumatic Stress Disorder: A Multisite ENIGMA-PGC Study: Subcortical Volumetry Results From Posttraumatic Stress Disorder Consortia. *Biol Psychiatry* **83**, 244-253, doi:10.1016/j.biopsych.2017.09.006 (2018).

8 Yehuda, R. Advances in understanding neuroendocrine alterations in PTSD and their therapeutic implications. *Ann N Y Acad Sci* **1071**, 137-166, doi:10.1196/annals.1364.012 (2006).

9 Milad, M. R. *et al.* Neurobiological basis of failure to recall extinction memory in posttraumatic stress disorder. *Biol Psychiatry* **66**, 1075-1082, doi:10.1016/j.biopsych.2009.06.026S0006-3223(09)00896-8 [pii] (2009).

10 Shin, L. M. *et al.* Exaggerated activation of dorsal anterior cingulate cortex during cognitive interference: a monozygotic twin study of posttraumatic stress disorder. *Am J Psychiatry* **168**, 979-985, doi:10.1176/appi.ajp.2011.09121812 (2011).

11 Goswami, S., Rodriguez-Sierra, O., Cascardi, M. & Pare, D. Animal models of post-traumatic stress disorder: face validity. *Frontiers in neuroscience* **7**, 89, doi:10.3389/fnins.2013.00089 (2013).

12 Deslauriers, J., Toth, M., Der-Avakian, A. & Risbrough, V. B. Current Status of Animal Models of Posttraumatic Stress Disorder: Behavioral and Biological Phenotypes, and Future Challenges in Improving Translation. *Biol Psychiatry* **83**, 895-907, doi:10.1016/j.biopsych.2017.11.019 (2018).

13 Flandreau, E. I. & Toth, M. Animal Models of PTSD: A Critical Review. *Current topics in behavioral neurosciences*, doi:10.1007/7854_2016_65 (2017).

14 Cohen, H. & Zohar, J. An animal model of posttraumatic stress disorder: the use of cut-off behavioral criteria. *Ann N Y Acad Sci* **1032**, 167-178 (2004).

15 Roelofs, K. Freeze for action: neurobiological mechanisms in animal and human freezing. *Philos Trans R Soc Lond B Biol Sci* **372**, doi:10.1098/rstb.2016.0206 (2017).

16 Fanselow, M. S. Neural organization of the defensive behavior system responsible for fear. *Psychon Bull Rev* **1**, 429-438, doi:10.3758/BF03210947 (1994).

17 Liang, Z., King, J. & Zhang, N. Uncovering intrinsic connectional architecture of functional networks in awake rat brain. *J Neurosci* **31**, 3776-3783 (2011).

18 Liang, Z., King, J. & Zhang, N. Anticorrelated resting-state functional connectivity in awake rat brain. *Neuroimage* **59**, 1190-1199, doi:S1053-8119(11)00896-2 [pii]10.1016/j.neuroimage.2011.08.009 (2012).

19 Ma, Z. *et al.* Functional atlas of the awake rat brain: A neuroimaging study of rat brain specialization and integration. *Neuroimage* **170**, 95-112, doi:10.1016/j.neuroimage.2016.07.007 (2018).

20 Ma, Z. & Zhang, N. Temporal transitions of spontaneous brain activity. *eLife* **7**, doi:10.7554/eLife.33562 (2018).

21 Gao, Y. R. *et al.* Time to wake up: Studying neurovascular coupling and brain-wide circuit function in the un-anesthetized animal. *Neuroimage*, doi:10.1016/j.neuroimage.2016.11.069 (2016).

22 Liang, Z., King, J. & Zhang, N. Intrinsic organization of the anesthetized brain. *J Neurosci* **32**, 10183-10191, doi:10.1523/JNEUROSCI.1020-12.2012 (2012).

23 Liang, Z., King, J. & Zhang, N. Neuroplasticity to a single-episode traumatic stress revealed by resting-state fMRI in awake rats. *Neuroimage* **103**, 485-491, doi:10.1016/j.neuroimage.2014.08.050 (2014).

24 Ubeda-Contreras, J., Marin-Blasco, I., Nadal, R. & Armario, A. Brain c-fos expression patterns induced by emotional stressors differing in nature and intensity. *Brain structure & function* **223**, 2213-2227, doi:10.1007/s00429-018-1624-2 (2018).

25 Janitzky, K., D'Hanis, W., Krober, A. & Schwegler, H. TMT predator odor activated neural circuit in C57BL/6J mice indicates TMT-stress as a suitable model for uncontrollable intense stress. *Brain Res* **1599**, 1-8, doi:10.1016/j.brainres.2014.12.030 (2015).

26 Daldrup, T., Lesting, J., Meuth, P., Seidenbecher, T. & Pape, H. C. Neuronal correlates of sustained fear in the anterolateral part of the bed nucleus of stria terminalis. *Neurobiology of learning and memory* **131**, 137-146, doi:10.1016/j.nlm.2016.03.020 (2016).

27 Gungor, N. Z. & Pare, D. CGRP inhibits neurons of the bed nucleus of the stria terminalis: implications for the regulation of fear and anxiety. *J Neurosci* **34**, 60-65, doi:10.1523/JNEUROSCI.3473-13.2014 (2014).

28 Da Cunha, C., Gomez, A. A. & Blaha, C. D. The role of the basal ganglia in motivated behavior. *Rev Neurosci* **23**, 747-767, doi:10.1515/revneuro-2012-0063 (2012).

29 Mitrofanis, J. Some certainty for the "zone of uncertainty"? Exploring the function of the zona incerta. *Neuroscience* **130**, 1-15, doi:10.1016/j.neuroscience.2004.08.017 (2005).

30 Hunt, A. J., Jr. *et al.* Paraventricular hypothalamic and amygdalar CRF neurons synapse in the external globus pallidus. *Brain structure & function* **223**, 2685-2698, doi:10.1007/s00429-018-1652-y (2018).

31 Paré, D. & Quirk, G. J. When scientific paradigms lead to tunnel vision: lessons from the study of fear. *npj Science of Learning* **2**, 6, doi:10.1038/s41539-017-0007-4 (2017).

32 Gruene, T. M., Flick, K., Stefano, A., Shea, S. D. & Shansky, R. M. Sexually divergent expression of active and passive conditioned fear responses in rats. *eLife* **4**, doi:10.7554/eLife.11352 (2015).

33 Holbrook, T. L., Hoyt, D. B., Stein, M. B. & Sieber, W. J. Perceived threat to life predicts posttraumatic stress disorder after major trauma: risk factors and functional outcome. *J Trauma* **51**, 287-292; discussion 292-283 (2001).

34 Yehuda, R. Current status of cortisol findings in post-traumatic stress disorder. *Psychiatr Clin North Am* **25**, 341-368, vii (2002).

35 Mouthaan, J. *et al.* The role of acute cortisol and DHEAS in predicting acute and chronic PTSD symptoms. *Psychoneuroendocrinology* **45**, 179-186, doi:10.1016/j.psyneuen.2014.04.001 (2014).

36 Rao, R. P., Anilkumar, S., McEwen, B. S. & Chattarji, S. Glucocorticoids protect against the delayed behavioral and cellular effects of acute stress on the amygdala. *Biol Psychiatry* **72**, 466-475, doi:10.1016/j.biopsych.2012.04.008 (2012).

37 McEwen, B. S. *et al.* Mechanisms of stress in the brain. *Nat Neurosci* **18**, 1353-1363, doi:10.1038/nn.4086 (2015).

38 Whitaker, A. M. & Gilpin, N. W. Blunted hypothalamo-pituitary adrenal axis response to predator odor predicts high stress reactivity. *Physiol Behav* **147**, 16-22, doi:10.1016/j.physbeh.2015.03.033 (2015).

39 Yehuda, R., McFarlane, A. C. & Shalev, A. Y. Predicting the development of posttraumatic stress disorder from the acute response to a traumatic event. *Biol Psychiatry* **44**, 1305-1313 (1998).

40 Delahanty, D. L., Raimonde, A. J. & Spoonster, E. Initial posttraumatic urinary cortisol levels predict subsequent PTSD symptoms in motor vehicle accident victims. *Biol Psychiatry* **48**, 940-947 (2000).

41 Weaver, I. C. *et al.* Reversal of maternal programming of stress responses in adult offspring through methyl supplementation: altering epigenetic marking later in life. *J Neurosci* **25**, 11045-11054, doi:10.1523/JNEUROSCI.3652-05.2005 (2005).

42 Cullinan, W. E., Herman, J. P., Battaglia, D. F., Akil, H. & Watson, S. J. Pattern and time course of immediate early gene expression in rat brain following acute stress. *Neuroscience* **64**, 477-505 (1995).

43 Dielenberg, R. A., Hunt, G. E. & McGregor, I. S. "When a rat smells a cat": the distribution of Fos immunoreactivity in rat brain following exposure to a predatory odor. *Neuroscience* **104**, 1085-1097 (2001).

44 Friedrich, R. W. Olfactory neuroscience: beyond the bulb. *Curr Biol* **21**, R438-440, doi:10.1016/j.cub.2011.04.036 (2011).

45 Ferrer, N. G. Efferent projections of the anterior olfactory nucleus. *J Comp Neurol* **137**, 309-320, doi:10.1002/cne.901370305 (1969).

46 Gozzi, A. *et al.* A neural switch for active and passive fear. *Neuron* **67**, 656-666, doi:10.1016/j.neuron.2010.07.008 (2010).

47 Kondoh, K. *et al.* A specific area of olfactory cortex involved in stress hormone responses to predator odours. *Nature* **532**, 103-106, doi:10.1038/nature17156 (2016).

48 Keay, K. A. & Bandler, R. Parallel circuits mediating distinct emotional coping reactions to different types of stress. *Neurosci Biobehav Rev* **25**, 669-678 (2001).

49 Walker, D. L. & Davis, M. Role of the extended amygdala in short-duration versus sustained fear: a tribute to Dr. Lennart Heimer. *Brain structure & function* **213**, 29-42, doi:10.1007/s00429-008-0183-3 (2008).

50 Somerville, L. H., Whalen, P. J. & Kelley, W. M. Human bed nucleus of the stria terminalis indexes hypervigilant threat monitoring. *Biol Psychiatry* **68**, 416-424, doi:10.1016/j.biopsych.2010.04.002 (2010).

51 Grupe, D. W. & Nitschke, J. B. Uncertainty and anticipation in anxiety: an integrated neurobiological and psychological perspective. *Nat Rev Neurosci* **14**, 488-501, doi:10.1038/nrn3524 (2013).

52 Davis, M. Neural systems involved in fear and anxiety measured with fear-potentiated startle. *Am Psychol* **61**, 741-756, doi:10.1037/0003-066X.61.8.741 (2006).

53 Dong, H. W. & Swanson, L. W. Projections from bed nuclei of the stria terminalis, posterior division: implications for cerebral hemisphere regulation of defensive and reproductive behaviors. *J Comp Neurol* **471**, 396-433, doi:10.1002/cne.20002 (2004).

54 Dong, H. W. & Swanson, L. W. Organization of axonal projections from the anterolateral area of the bed nuclei of the stria terminalis. *J Comp Neurol* **468**, 277-298, doi:10.1002/cne.10949 (2004).

55 Tovote, P., Fadok, J. P. & Luthi, A. Neuronal circuits for fear and anxiety. *Nat Rev Neurosci* **16**, 317-331, doi:10.1038/nrn3945 (2015).

56 Sierra-Mercado, D., Padilla-Coreano, N. & Quirk, G. J. Dissociable roles of prelimbic and infralimbic cortices, ventral hippocampus, and basolateral amygdala in the expression and extinction of conditioned fear. *Neuropsychopharmacology* **36**, 529-538, doi:10.1038/npp.2010.184 (2011).

57 Vertes, R. P. & Kocsis, B. Brainstem-diencephalo-septohippocampal systems controlling the theta rhythm of the hippocampus. *Neuroscience* **81**, 893-926 (1997).

58 Buzsaki, G. Theta oscillations in the hippocampus. *Neuron* **33**, 325-340 (2002).

59 Lesting, J. *et al.* Directional theta coherence in prefrontal cortical to amygdalo-hippocampal pathways signals fear extinction. *PLoS One* **8**, e77707, doi:10.1371/journal.pone.0077707 (2013).

60 Marek, R. *et al.* Hippocampus-driven feed-forward inhibition of the prefrontal cortex mediates relapse of extinguished fear. *Nat Neurosci* **21**, 384-392, doi:10.1038/s41593-018-0073-9 (2018).

61 Zhang, J. *et al.* Decreased gray matter volume in the left hippocampus and bilateral calcarine cortex in coal mine flood disaster survivors with recent onset PTSD. *Psychiatry Res* **192**, 84-90, doi:10.1016/j.pscychresns.2010.09.001 (2011).

62 Lebow, M. A. & Chen, A. Overshadowed by the amygdala: the bed nucleus of the stria terminalis emerges as key to psychiatric disorders. *Molecular psychiatry* **21**, 450-463, doi:10.1038/mp.2016.1 (2016).

63 Zohar, J. *et al.* High dose hydrocortisone immediately after trauma may alter the trajectory of PTSD: interplay between clinical and animal studies. *European neuropsychopharmacology : the journal of the European College of Neuropsychopharmacology* **21**, 796-809, doi:10.1016/j.euroneuro.2011.06.001 (2011).

64 Schelling, G., Roozendaal, B. & De Quervain, D. J. Can posttraumatic stress disorder be prevented with glucocorticoids? *Ann N Y Acad Sci* **1032**, 158-166, doi:10.1196/annals.1314.013 (2004).

65 King, J. A. *et al.* Procedure for minimizing stress for fMRI studies in conscious rats. *J Neurosci Methods* **148**, 154-160 (2005).

66 Bergmann, E., Zur, G., Bershadsky, G. & Kahn, I. The Organization of Mouse and Human Cortico-Hippocampal Networks Estimated by Intrinsic Functional Connectivity. *Cereb Cortex* **26**, 4497-4512, doi:10.1093/cercor/bhw327 (2016).

67 Yoshida, K. *et al.* Physiological effects of a habituation procedure for functional MRI in awake mice using a cryogenic radiofrequency probe. *J Neurosci Methods* **274**, 38-48, doi:10.1016/j.jneumeth.2016.09.013 (2016).

68 Chang, P. C. *et al.* Novel method for functional brain imaging in awake minimally restrained rats. *J Neurophysiol* **116**, 61-80, doi:10.1152/jn.01078.2015 (2016).

69 Liang, Z., Liu, X. & Zhang, N. Dynamic resting state functional connectivity in awake and anesthetized rodents. *Neuroimage* **104**, 89-99, doi:10.1016/j.neuroimage.2014.10.013 (2015).

70 Power, J. D., Barnes, K. A., Snyder, A. Z., Schlaggar, B. L. & Petersen, S. E. Spurious but systematic correlations in functional connectivity MRI networks arise from subject motion. *Neuroimage* **59**, 2142-2154, doi:10.1016/j.neuroimage.2011.10.018 (2012).

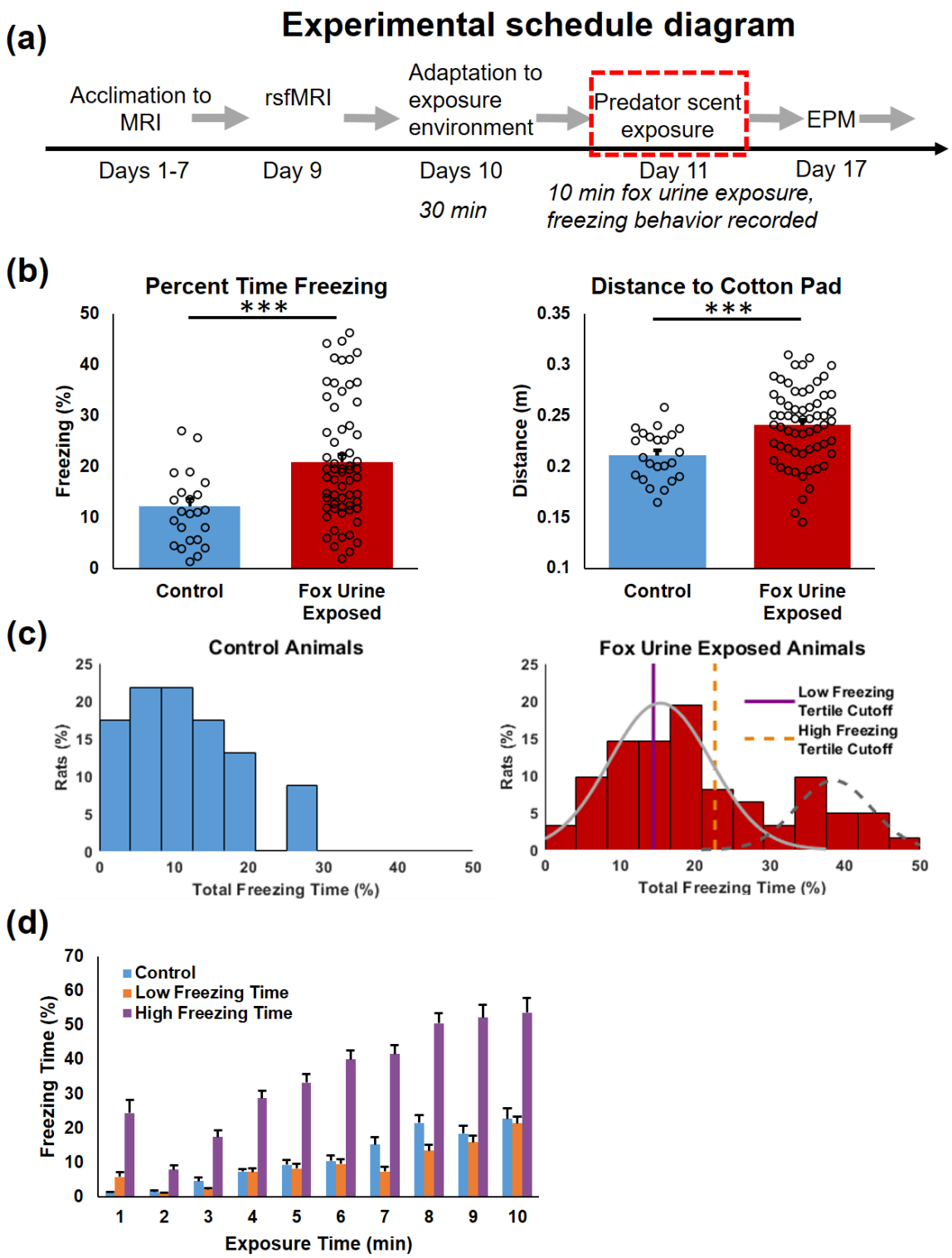

Figure 1. Freezing time during the 10-min exposure session in control (n = 23) and fox urine exposed (n = 62) groups. **a**) Diagram of experimental schedule. **b**) Fox urine exposed animals showed a significantly longer freezing time (left, $p < 0.0005$, in percentage) and greater mean distance (right, $p < 0.0007$, in meters) from the cotton

pad than controls. **c**) The distributions of individual animals' freezing time in the control group (left) and the exposed group (right) displayed as probability histograms. The freezing time distribution in exposed animals was fit to a Gaussian mixture model which demonstrated a bimodal distribution. **d**) Freezing time each min plotted as a function of time in low-freezing (n=21), high-freezing (n=21) and control animals during fox urine exposure. The high freezing animals displayed higher freezing phenotype during the first minute of exposure, with a significantly longer freezing time than both low freezing and control animals from the 1st minute through the 10th minute ($p < 0.005$ for each minute of exposure).

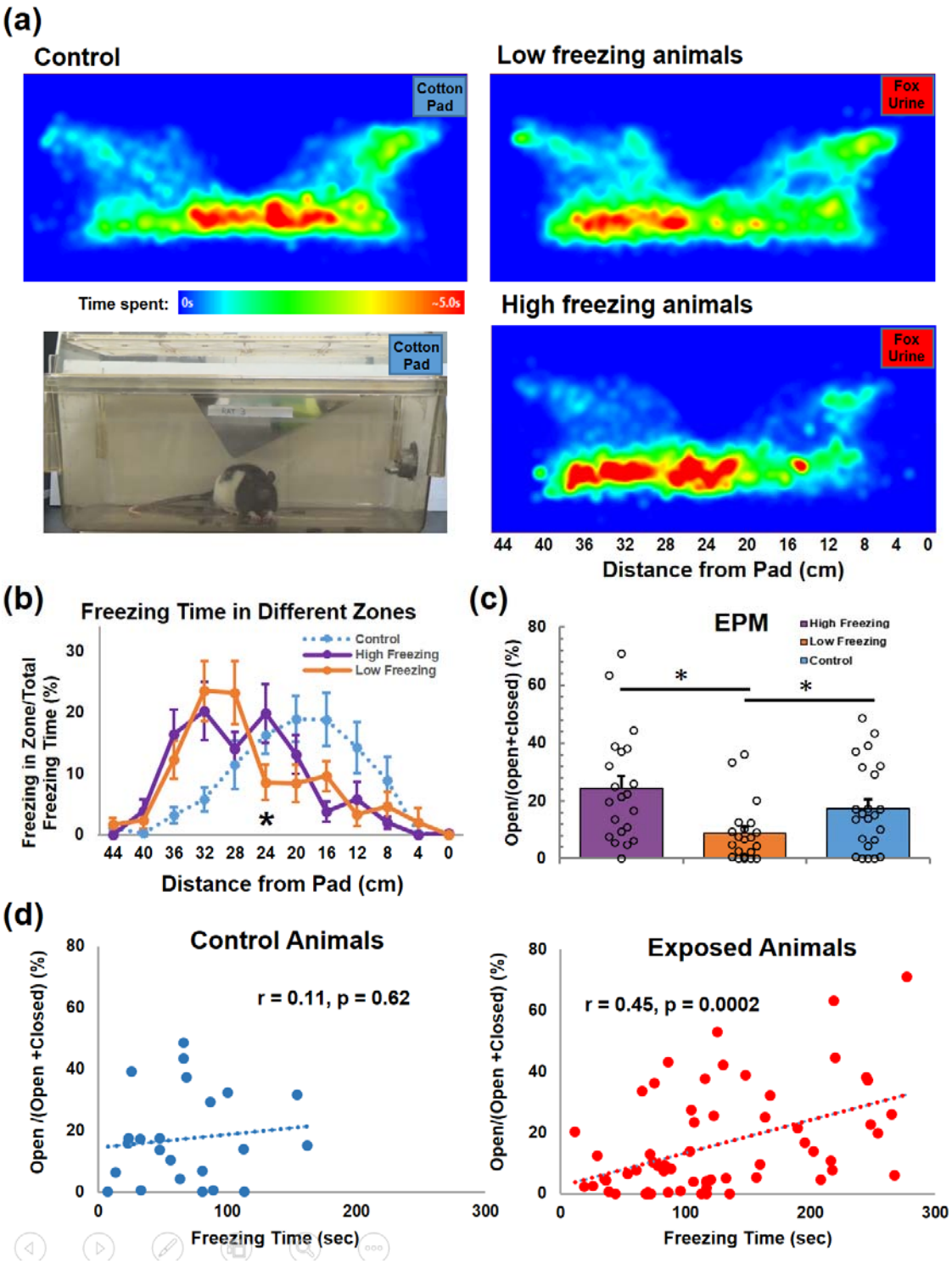

Figure 2. Low-freezing animals exhibited stronger stress response during fox urine exposure and higher anxiety 6 days after exposure. **a**) Heat maps of the total time at each location for the control, low freezing, and high freezing groups. The control group showed no evident bias for either side of the cage. The low freezing group showed a strong bias toward the far end (from the pad) of the cage, while the high freezing rats

also showed a bias toward the far end of the cage, but to a less extent. **b**) The distribution of the percent freezing time for each group across the cage, which was divided into 12 even-size zones. The x-axis indicates the distance to the pad from the center of each zone. Similar to the distributions of total time spent, the percent freezing time in control rats displayed little bias for either side of the cage. High and low freezing animals showed a bias of percentage freezing time toward the far end of the cage, with the low-freezing rats showing even stronger bias than high-freezing animals, evidenced by significantly lower percent freezing time of the low-freezing group in the zone 24 cm away from the pad compared to the high-freezing group ($p = 0.026$). **c**) Elevated plus maze performed 6 days post exposure in all three groups of animals. The high-freezing group showed significantly higher EPM score (open/open+closed arm time) compared to the low-freezing group ($p < 0.002$). Low freezing animals also showed a significantly lower EPM score compared to controls ($p < 0.04$), while no significant difference was seen between control and high freezing groups. **d**) The freezing time was positively correlated to the EPM score across all exposed animals ($r = 0.45$, $p = 0.0002$), but not control animals ($r = 0.11$, $p = 0.62$).

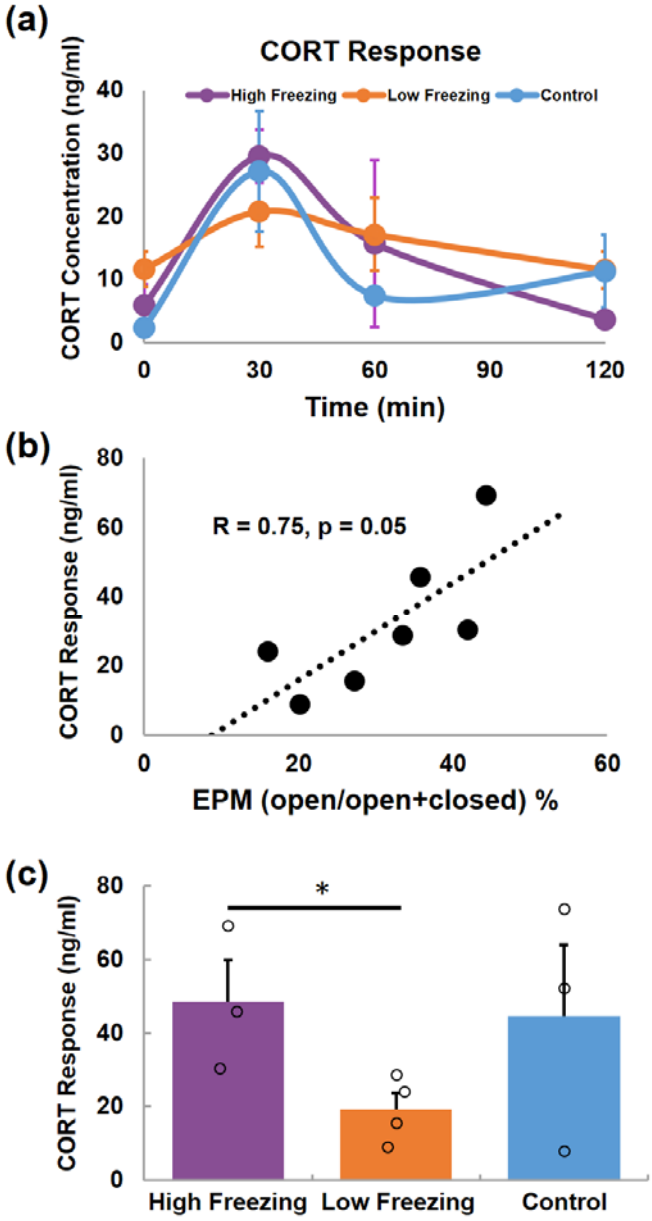

Figure 3. Corticosterone response to fox urine exposure. **a**) The time course of corticosterone (in ng/ml) for high-freezing, low-freezing and control animals. **b**) Significant correlation (p = 0.05) between the CORT responsiveness (y-axis) and EPM score (open/open+closed arm time, x-axis, measured 6 days post exposure) for high- and low-freezing animals. CORT responsiveness took into account both the rise and fall around the peak hormonal response (30 min). **c**) CORT responsiveness in all three groups. High- and low-freezing animals showed a significant difference in the CORT responsiveness (p = 0.043).

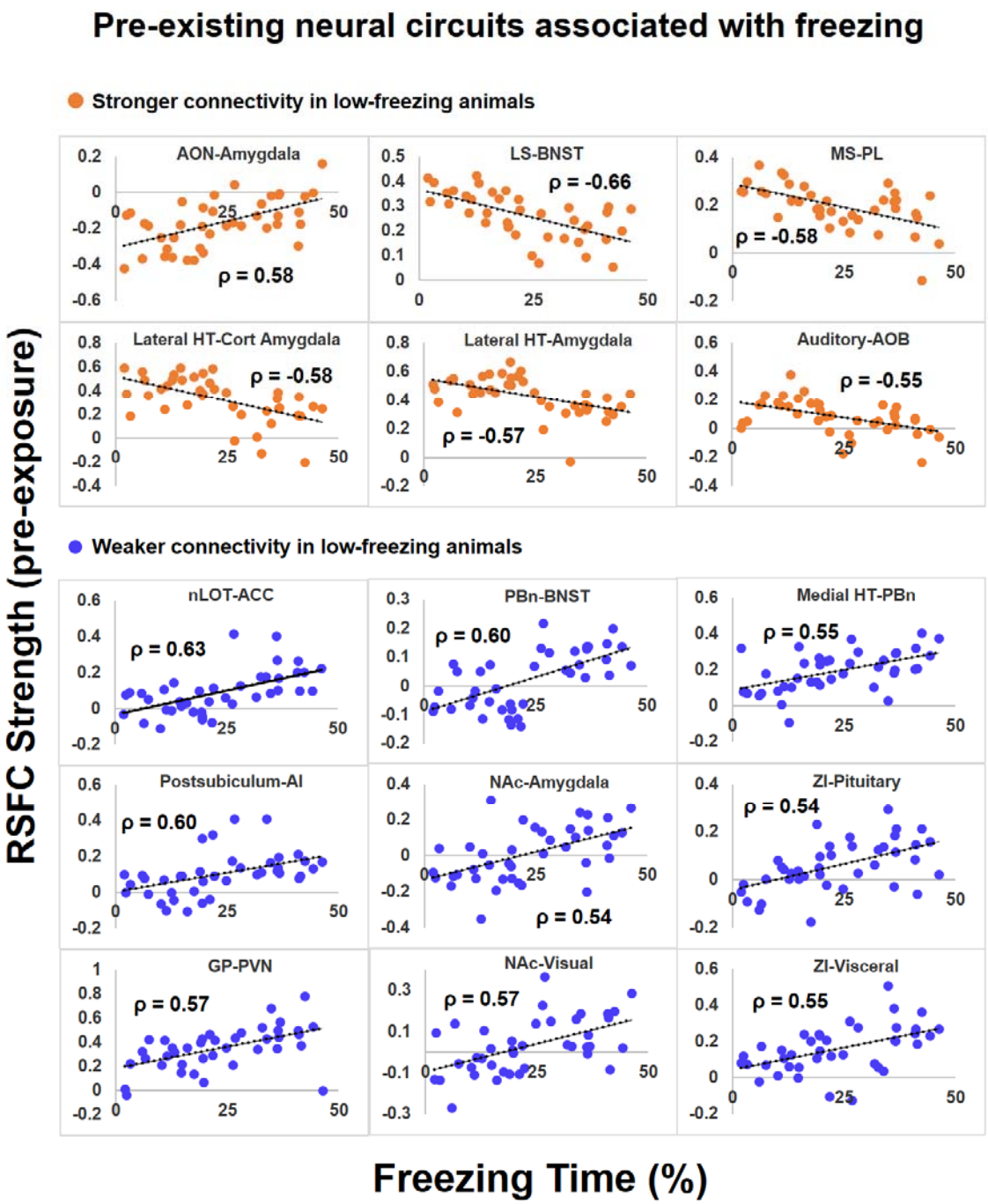

Figure 4. Neural circuits with pre-trauma resting-state functional connectivity (y-axis) correlated ($p<0.05$, FDR corrected) with percentage freezing time (x-axis) in all fox urine exposed animals (n=62). AON, anterior olfactory nucleus; LS, lateral septum; BNST, bed nucleus of the stria terminalis; MS, medial septum; PL, prelimbic cortex; HT, hypothalamus; Cort Amygdala, cortical amygdala; AOB, accessory olfactory Bulb; nLOT, lateral olfactory tract nucleus; ACC, anterior cingulate cortex; PBn, parabrachial nucleus; AI, postsubiculum-agranular insula; NAc, nucleus accumbens; ZI, zona inserta; GP, globus pallidus; PVN, paraventricular nucleus.

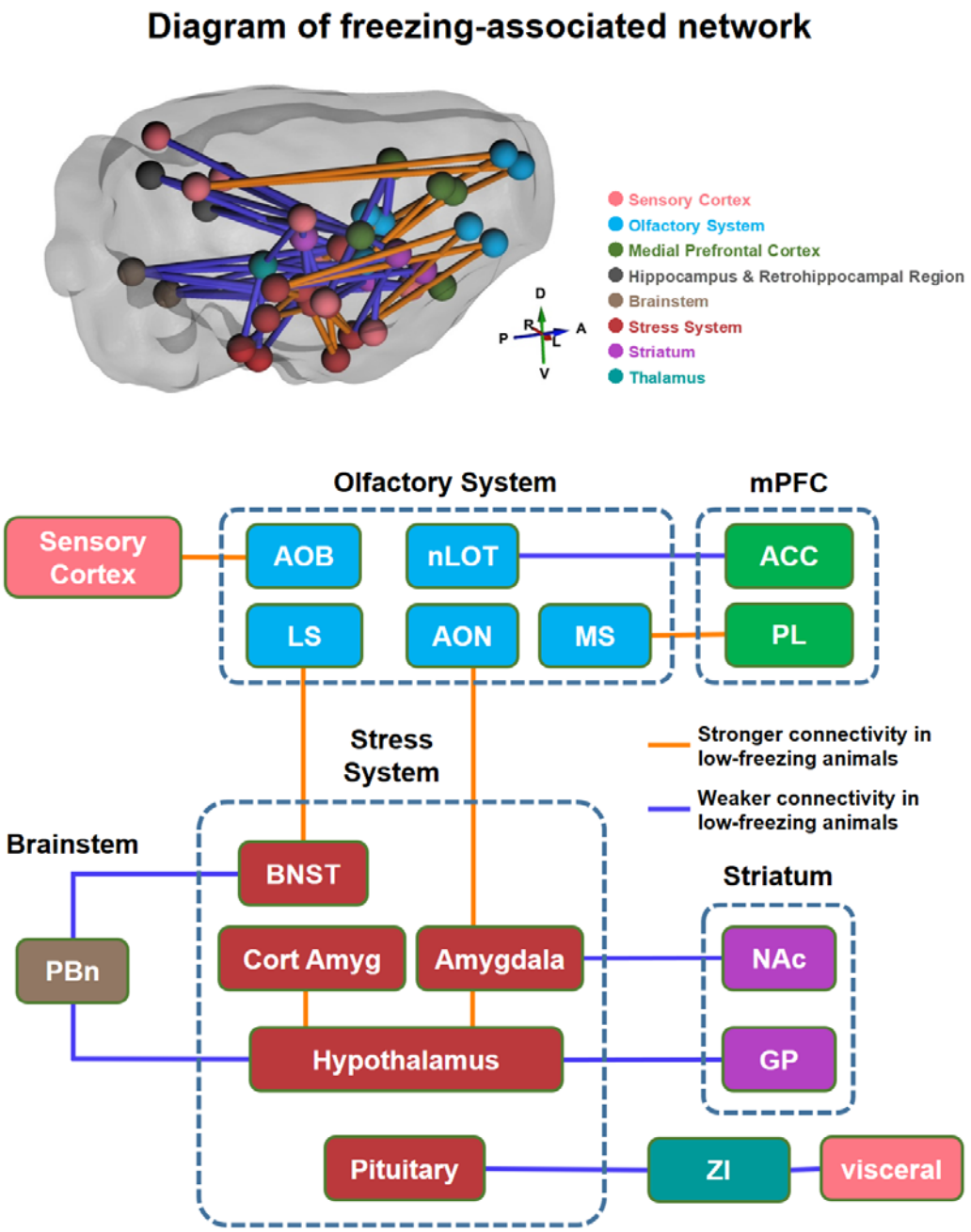

Figure 5. Diagram of freezing-associated neural network, including neural circuits showing significant correlation between pre-trauma RSFC and total freezing time shown in Fig. 4. Brain regions are grouped and color coded based on the brain systems they belong to. Orange lines indicate stronger connectivity in low-freezing animals. Blue lines indicate weaker connectivity in low-freezing animals. See the caption of Fig. 4 for the abbreviation.